Todd G. Nelson[1]
Department of Mechanical Engineering,
Brigham Young University,
Provo, UT 84602
e-mail: toddgn@byu.edu

Robert J. Lang
Lang Origami,
Alamo, CA 94507

Nathan A. Pehrson
Department of Mechanical Engineering,
Brigham Young University,
Provo, UT 84602

Spencer P. Magleby
Department of Mechanical Engineering,
Brigham Young University,
Provo, UT 84602

Larry L. Howell
Department of Mechanical Engineering,
Brigham Young University,
Provo, UT 84602

Facilitating Deployable Mechanisms and Structures Via Developable Lamina Emergent Arrays

A method is presented utilizing networks of lamina emergent joints, known as lamina emergent arrays, to accommodate large-curvature developable structures suited to deployable applications. By exploiting the ruling lines in developable surfaces, this method enables developable structures and mechanisms that can be manufactured with two-dimensional geometry and yet have a greater range of elastic motion than is possible with a solid sheet of material. Aligning the joints to the ruling lines also biases the structure to a specific deployment path. A mathematical model is developed to describe the resulting stiffness of the structure employing the lamina emergent arrays and equations are derived to facilitate stress analysis of the structure. Finite element results show the sensitivity of alignment of the elements in the array to the stress present in the developed structure. A specific technique for creating an array pattern for conical developable surfaces is described. Examples of developable structures and mechanisms, including curved-fold origami models transitioned to thick materials and two origami-inspired mechanisms, are examined. [DOI: 10.1115/1.4031901]

Keywords: developable, deployable, curved folding, origami, lamina emergent, 3D printing

1 Introduction

The objective of this work is to create a method to mathematically model and design large-curvature, developable structures suited to deployable applications using lamina emergent arrays. These arrays are networks of lamina emergent joints, which are compliant joints made from a single layer of material. The research enables the construction of developable surfaces in thick or brittle materials which often reside outside the design space when working with sheet material. It also explores how greater elastic deflection can be achieved in sheet products. This increased deflection lends itself toward deployable mechanisms requiring large elastic deflection. These networks of lamina emergent joints can also create a structure that is biased to move along a specific deployment path.

Developable surfaces have emerged as subjects of interest not only to mathematicians, but engineers and artists as flat sheets are morphed into intriguing and complex shapes which can be used in automobiles, boats, architecture, furniture, and clothing construction. Developable surfaces also take a prominent place in origami, specifically curved-fold origami. However, the transition between the mathematical descriptions and paper-thin origami into engineering materials and structures presents some unique challenges. These challenges include the high bending stresses that develop when a thick, stiff material is bent to form the desired developable surface. These bending stresses can be reduced by using arrays of previously developed torsional and bending joints. Furthermore, particular placement of the torsion hinge axes along the ruling lines of the developable surface results in a configuration where stresses are reduced effectively. This method thus extends the range of elastic motion for engineering materials utilized in deployable mechanisms and creates a structure that is inclined to move into a specific shape.

[1]Corresponding author.
Manuscript received June 30, 2015; final manuscript received October 14, 2015; published online March 7, 2016. Assoc. Editor: Mary Frecker.

2 Background

2.1 Developable Surfaces. A developable surface is formed from a flat plane by the process of bending, but not stretching or shrinking [1]. Leonhard Euler and Gaspard Monge pioneered the first of many studies of these intriguing surfaces [2,3]. These surfaces possess the attribute of being isometric, meaning that a distance between two points on the flat undeveloped plane will be equivalent to the distance between the two corresponding points on the developed surface [1]. Developable surfaces are a subset of ruled surfaces when limited to R^3 space [4]. Ruled surfaces are characterized by the quality that for each point on the surface there exists a straight line, known as a ruling line or generating line, lying upon the surface through the point. The ruling line does not need to characterize one of the principle curvatures at the point in a ruled surface. However, for the surface to be developable, the additional constraint is imposed that the ruling line must be one of the principle curvatures. This leads to the useful mathematical definition of a developable surface that the Gaussian curvature, or product of the two principle curvatures, at all points of a developable surface is zero. Another alternative but useful definition of a developable surface is the normal of the tangent plane to the surface does not change direction when moving along the ruling lines [1]. Finally, a developable surface can be considered the envelope of a one-parameter family of planes [1].

In addition to the trivial case of the plane, there are three fundamental classes of developable surfaces: generalized cylinders, generalized cones, and tangent developed [5]. These are also referred to as torsal ruled surfaces and are shown in Fig. 1. Generalized cylinders contain ruling lines parallel to each other. Generalized cones contain ruling lines which meet at a point on or off the actual surface. Tangent developed surfaces consist of ruling lines that correspond to the family of tangent lines of a space curve. More complex developable surfaces can be created by combining the different classes [4]. This is achieved by joining a developable patch of a certain class to another by aligning the ruling lines [6] or reflection of a patch across the osculating plane at each point in a crease [7]. Combinations of torsal ruled surfaces

 Copyright © 2016 by ASME

Downloaded From: http://asmedigitalcollection.asme.org/ on 03/07/2016 Terms of Use: http://www.asme.org/about-asme/terms-of-use

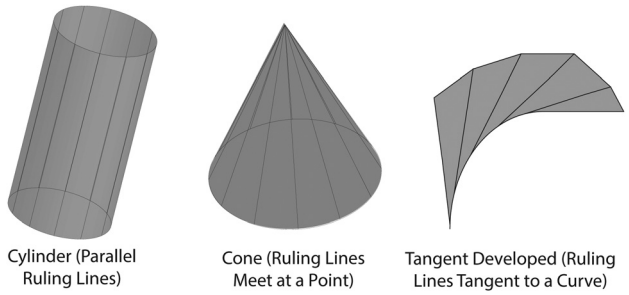

Fig. 1 The three classes of developable surfaces: cylinder (left), cone (middle), and tangent developed (right)

which retain the property of being developable have been named discrete developable surfaces, composite developable surfaces, or general developable surfaces [8–10] (Fig. 2).

Curved-crease origami is intrinsically tied to developable surfaces because curved creases tie together developable patches. While much of the field of curved folding is yet unexplored, a summary of curved folding research is set forth in an article by Demaine et al. [11] and some of the best known curved folding work comes from David Huffman [12] and Ron Resch [13]. Mathematical descriptions of curved folding were furthered by Fuchs et al. [7] and Duncan et al. [14]. Recently, David Huffman's work has been further analyzed by Demaine et al. and new insights into the design of curve-folded origami have been explained [15–17].

2.2 Lamina Emergent Mechanisms (LEMs). Like developable surfaces, LEMs are also formed from the flat plane. LEMs are defined as mechanical devices fabricated from planar materials (laminae) with motion that emerges out of the fabrication plane [18]. These mechanisms draw upon flexibility to achieve their motion and are therefore considered a subset of compliant mechanisms, or mechanisms that use flexible members to achieve at least some of their mobility [19]. The main benefits of the LEMs include planar fabrication, easily scalable to the microlevel, reduced part counts, lack of friction contacts, and a compact size.

Delimont et al. explored various types of joints suitable for LEMs [20,21], particularly for origami-inspired mechanisms. This study utilizes several of these joints in specific arrays to create developable surfaces. These joints exhibit a primary motion similar to folding and can be manufactured using two-dimensional geometry. The joints have been modeled with an equivalent stiffness, K_{eq}, to represent the rotational stiffness about the joint where

$$K_{eq}\theta = T \tag{1}$$

with T being the torque applied across the joint and θ is the angular deflection of the joint.

A summary will be presented of the geometry and equations of seven joints. Six of the joints are pictured in Fig. 3 and the seventh joint is a simple groove joint. Figure 4 shows the parameters connecting the equations and the geometry for two of the joints.

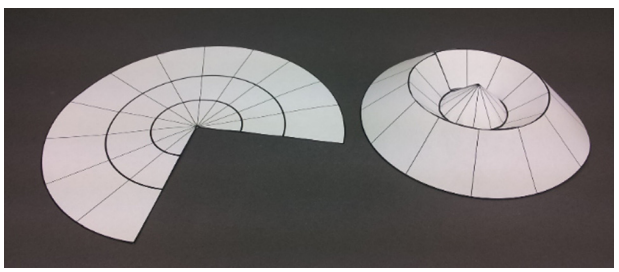

Fig. 2 Example of a general developable surface in an unfolded and folded configuration with ruling lines shown

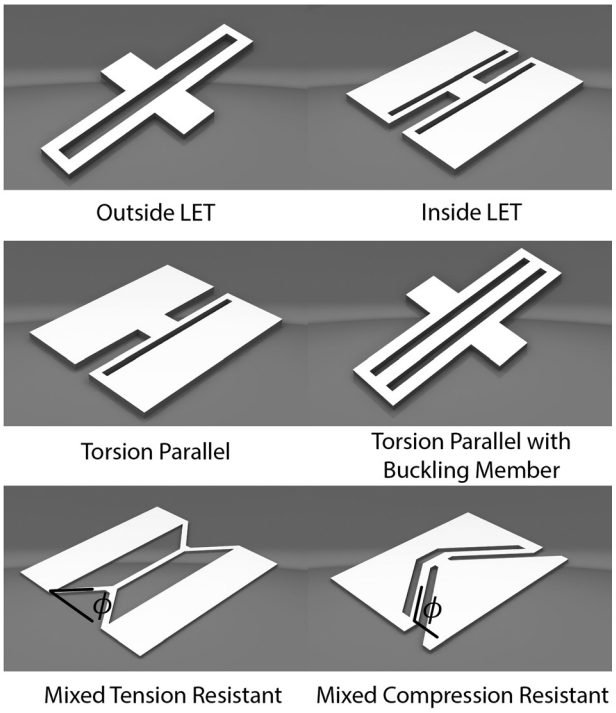

Fig. 3 A sample of joints suitable for constructing developable surfaces

While the geometry of the other joints is defined similarly, the reader is referred to the literature [20,21] for further clarification of the parameters of the joints not shown in Fig. 4.

2.2.1 The Outside LET Joint. The outside lamina emergent torsional (LET) joint shown in Figs. 3 and 4 enables large angles of rotation in its primary folding direction but is subject to

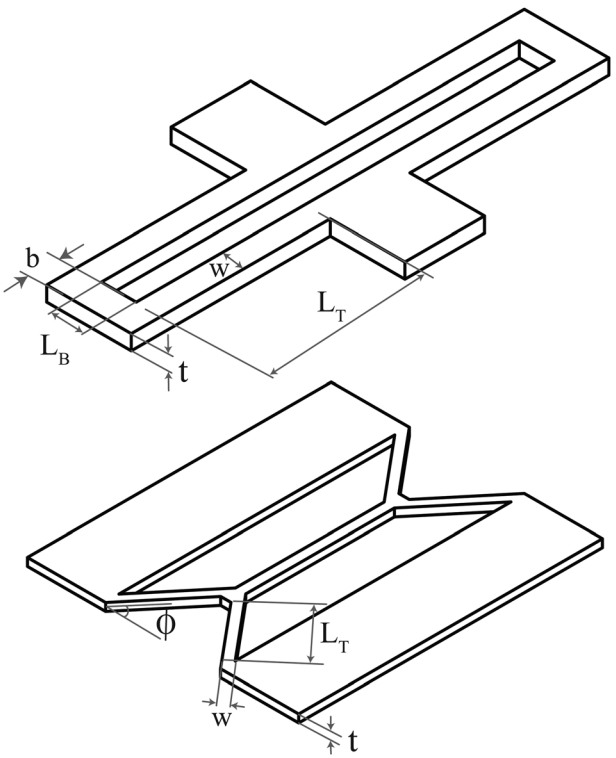

Fig. 4 Geometric parameters for the outside LET and mixed tension resistant joints

Downloaded From: http://asmedigitalcollection.asme.org/ on 03/07/2016 Terms of Use: http://www.asme.org/about-asme/terms-of-use

secondary motions of torsion, lateral bending, compression, and tension. It does not have a stable center of rotation in folding. Jacobsen et al. [22] developed a spring model of the joint for a folding motion to find an equivalent stiffness. The equivalent stiffness can be expressed as

$$K_{\text{eq}} = \frac{2K_B K_T}{2K_B + K_T} \tag{2}$$

The spring constant of the torsion legs, K_T, is

$$K_T = \frac{Gwt^3\left(\frac{1}{3} - 0.21\frac{t}{w}\left(1 - \frac{t^4}{12w^4}\right)\right)}{L_T} \tag{3}$$

where $w \geq t$ and G is the shear modulus.

The spring constant of the bending area, K_B, is given by

$$K_B = \frac{EI}{L_B} \text{ with } I = \frac{bt^3}{12} \tag{4}$$

2.2.2 The Inside LET Joint. The inside lamina emergent (LET) joint shown in Fig. 3 also exhibits torsion, lateral bending, compression, and tension as secondary motions while allowing for large deflections in the folding motion. With large magnitudes of compression or tension, the inside LET shows a stiffer response than the outside LET. The spring model for the inside LET yields an equivalent stiffness expressed as

$$K_{\text{eq}} = \frac{K_B K_T}{K_B + K_T} \tag{5}$$

where K_T and K_B are given by Eqs. (3) and (4).

2.2.3 Torsion Parallel Joint. The torsion parallel joint shown in Fig. 3 shows an increased stiffness in tension and compression when compared to the outside or inside LET joints and also provides a more fixed center of rotation. The stiffness of this joint in folding is given by

$$K_{\text{eq}} = \frac{2K_T K_B}{K_B + K_T} \tag{6}$$

where K_T and K_B are given by Eqs. (3) and (4).

2.2.4 Torsion Parallel With Buckling Member Joint. The torsion parallel with buckling member joint shown in Fig. 3 provides better resistance to tension and compression loads as compared to the inside and outside LET joints by the addition of a member to withstand a buckling motion induced by the loads. The equivalent stiffness of the joint in folding reduces to the same formula as the inside LET joint as shown in Eq. (5) with K_T and K_B being described by Eqs. (3) and (4).

2.2.5 Mixed Tension Resistant Joint. The mixed tension resistant joint, where ϕ ranges from 0 to $\pi/2$ radians, is depicted in Fig. 3. This joint is useful when greater resistance to tension than compression is desirable. The stiffness can be characterized by the following equation with ϕ in radians:

$$K_{\text{eq}} = \left|1 - \frac{2\phi}{\pi}\right|^{0.1096} K_B \cos^2\phi + K_T \sin^2\phi \tag{7}$$

with K_B and K_T given by

$$K_B = \frac{2\rho\text{EI}}{L_T} \text{ with } I = \frac{wt^3}{12} \tag{8}$$

$$K_T = \frac{2Gwt^3\left(\frac{1}{3} - 0.21\frac{t}{w}\left(1 - \frac{t^4}{12w^4}\right)\right)}{L_T} \tag{9}$$

In these equations, ρ is commonly approximated as 1.5164 [21], w is the width, and t is the thickness of the compliant section with $w \geq t$, E is Young's modulus, G is the shear modulus, and L_T is the length of the compliant section.

2.2.6 Mixed Compression Resistant Joint. When a stiffer resistance to compression is desired, the mixed compression resistant joint as shown in Fig. 3 is a good candidate. The stiffness of this joint can also be described by Eqs. (7)–(9) where ϕ ranges from $\pi/2$ to π radians.

2.2.7 Groove Joint. The groove joint is simply an area of reduced cross section in a panel and is simple to create. The center of rotation on a groove joint is relatively stable throughout its bending motion. A living hinge can be considered as a groove joint with a very small stiffness in bending. The expression for the equivalent stiffness of the groove joint is

$$K_{\text{eq}} = \frac{GWH^3\left(\frac{1}{3} - 0.21\frac{H}{W}\left(1 - \frac{H^4}{12W^4}\right)\right)}{L} \tag{10}$$

where G is the shear modulus, H is the height of the groove, L is the depth of the groove, and W is the length of the groove and panel. For a diagram of these parameters, the reader is referred to the literature [21].

2.3 Current and Past Applications. Previous research has yielded intriguing methods to create 3D geometry from sheet material. One of the oldest methods of creating 3D structures from sheet material is origami. Origami uses combinations of paper folds to create a 3D structure. You [23] discussed the advantages and challenges of origami in creating folding structures. Dureisseix [24] presented an overview of how origami patterns have been applied in engineering applications, such as deployable structures. Cylinders, spirals, and bi-directional sheets were created using microassembly techniques based on origami by Jamal et al. [25]. Origami metamaterials were investigated by Silverberg et al. [26]. Lee et al. [27] explored how the origami waterbomb base could be utilized as a dynamic wheel structure. Energy absorption applications in crushing of thin walled square tubes with origami structures was analyzed by Ma et al. [28]. An interesting method of self-folding origami structures from thin polymer material and controlled heat absorption was presented by Liu et al. [29]. A self folding robot was created by Felton et al. [30]. Kirigami techniques have been used to investigate the creation of custom honeycomb cross sections from flat sheets [31]. Miyashita et al. [32] used self folding with curved creases to create propellers and Gattas et al. [33] explored how curved creases and panels can be used in Miura-derivative prismatic base patterns.

Construction of developable surfaces has received attention from a variety of industries, including ship building, automotive, architecture, clothing and footwear, computer animation, and image processing. A process of designing shoe uppers using triangles and optimizing the surface to make it more developable has been explained by Chung et al. [34]. Kilian et al. [35] created an algorithm to approximate a nearly developable structure as a combination of developable patches, culminating in a case study of a fully developable car body. Pottmann et al. [36] approximated freeform architectural surfaces by using developable panels connected together. Further approximation of freeform surfaces was explored using single and doubly curved panels by Eigensatz et al. [37].

This research presents a novel method of creating developable surfaces that will enable many of these processes to be applied to thicker materials in addition to allowing a greater elastic range of motion.

3 Method

Each of the joints discussed in Sec. 2.2 can be considered as the fundamental unit of an array. These units can be connected

Downloaded From: http://asmedigitalcollection.asme.org/ on 03/07/2016 Terms of Use: http://www.asme.org/about-asme/terms-of-use

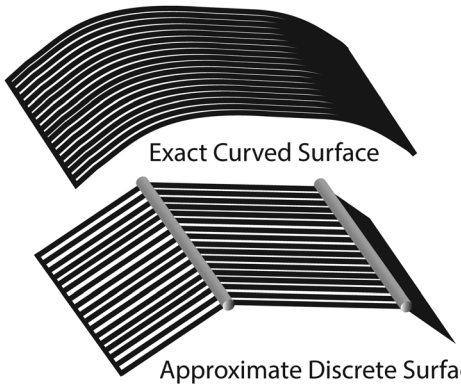

Fig. 5 Discretized surface model using hinges and panels

together in parallel, series, or a combination of both. Deployable developable surfaces, that is, surfaces which can move back and forth between a flat configuration and a developed surface without yielding, can be created with these joint arrays. It should be noted that while deployable structures normally lock into two positions, the surfaces created by these joint arrays have a single stable position to which the surface wants to return. Additional hardware could be used to lock the surface into the deployed shape. Only an approximation of the surface is possible because the joint arrays cannot create a smooth curved surface but rather a discrete approximation of a surface. This discretization can be roughly modeled as a series of pin joints and rigid panels as shown in Fig. 5.

While the design space for arrays of joints used to form a deployable developable surface is vast, several unique properties of developable surfaces cause one specific arrangement to stand out as particularly efficient in terms of achieving the elastic deflection while maintaining stresses below the strength of the material. This configuration consists of aligning the folding axis of the joints to the rules of the developable surface. When the joints are arranged in this fashion, the direction of the primary motion of each joint is matched to the most extreme curvature of the surface. This result can be seen from the following informal proof. At each point of a developable surface the Gaussian curvature vanishes, or restated, the Gaussian curvature is equal to zero. Because the Gaussian curvature is the product of the two principal curvatures, one can see that at least one of the principal curvatures at any point is also equal to zero. The direction of this principal curvature corresponds to the direction of the ruling line. As is discussed in Ref. [38], the directions of the principal curvatures are orthogonal at any point. Thus the direction of the other principal curvature is orthogonal to the ruling line. The implementation of this method can be seen in Fig. 6, where torsion joints of a Mobius strip are not aligned (*a*) and then aligned to the rules (*b*).

A finite element analysis (FEA) was performed to investigate the sensitivity of the stress caused by bending to the alignment the joints along the ruling lines of developable surfaces with parallel

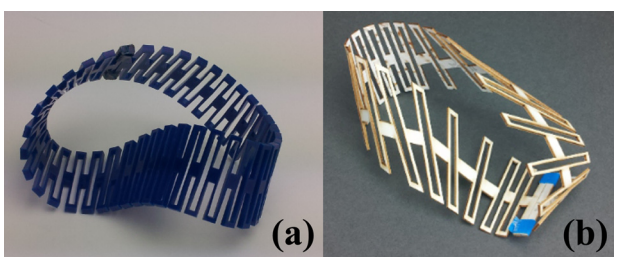

Fig. 6 Illustration of the method of aligning the axes of the joints to the ruling lines in a Mobius strip: (*a*) before alignment and (*b*) after alignment

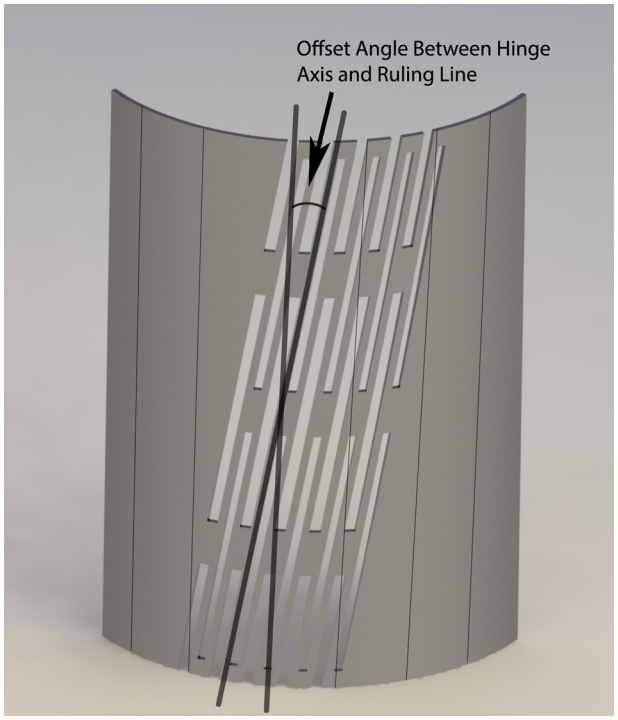

Fig. 7 Computer-aided design (CAD) model used in FEA to determine the sensitivity of hinge axis alignment to parallel ruling lines

ruling lines. An array of torsional joints was created as shown in Fig. 7 with a thickness of 1.143 mm (0.045 in.) and torsion bars 22.225 mm (0.875 in.) long with a width of 1.651 mm (0.065 in.). An isotropic material with a modulus of 207 GPa (30×10^6 psi) and Poisson's ratio of 0.3 was used. Twelve models were created by varying the angle of the torsional joint axes as measured from the parallel ruling lines from 0 to 20 deg in increments of 2 deg. Using ANSYS (Shell 181) the models were fully fixed at one edge and a displacement load of 7.62 mm (0.3 in.) was applied to the opposite edge. The models were stress converged to within a 10% change of Von Mises maximum stress.

A graph of the maximum Von Mises stress for each of the models is shown in Fig. 8 along with a reference line which shows the maximum stress of a solid plate without a torsional joint array moved through the same displacement. Images of three cases of the joint arrays (0, 10, and 20 deg offsets) are shown in Fig. 9. As expected from studies of shear stresses in rectangular torsional

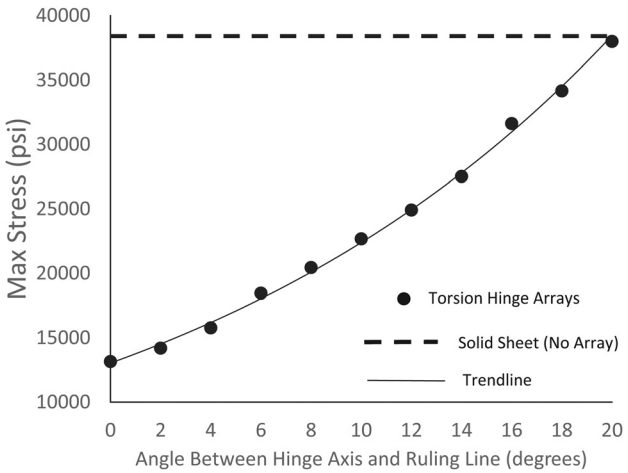

Fig. 8 Von Mises stress sensitivity to hinge axis alignment for parallel ruling lines

Downloaded From: http://asmedigitalcollection.asme.org/ on 03/07/2016 Terms of Use: http://www.asme.org/about-asme/terms-of-use

bars, the maximum stress in the 0 deg offset occurs on the outside of the middle of the wider side of the rectangular torsional beam. In the 10 deg offset model, the maximum shear stress has changed locations and occurs at the base of the torsional bar reflecting a stress concentration that has developed due to the hinge axis and ruling line offset. Further, in the 20 deg offset model the maximum stress location has changed to the second torsion member and is similar to the location of the maximum stress of a cantilever beam in bending. As the offset is increased from 0 to 20 deg, the stresses grow in an exponential manner with an R^2 value of 0.9976.

By using joints which have one axis that is markedly less stiff than any other direction, an array which is aligned to a particular ruling will resist moving away from the path of developable shapes characterized by that ruling during the array's deployment. It may be possible to quantify this reluctance toward deviation from the path through energy methods or through characterizing the stiffness of the arrays for motions other than the primary folding motion.

4 Mathematical Model

A relatively straightforward mathematical model was created to describe how arrays of joints function when aligned with the rules of a developable surface. If each joint unit is considered as a torsional spring with a stiffness, K_{eq}, as described for each type of joint in Sec. 2.2, then arrays of these joints can be modeled as a network of torsional springs in parallel and series. Joints placed along a single ruling line can be considered as torsional springs placed in a parallel arrangement. This can be described by

$$K_p = \sum_{i=1}^{m} K_{eq,i} \tag{11}$$

where K_p is the equivalent stiffness of all the joints along the ruling line, m is the number of joints along the ruling line, and $K_{eq,i}$ is the stiffness of the ith joint along the ruling line.

When multiple ruling lines contain joints K_{tot}, the total stiffness of the array in bending can be found using

$$\frac{1}{K_{tot}} = \sum_{j=1}^{n} \frac{1}{K_{p,j}} \tag{12}$$

where n is the number of ruling lines which contain joints and $K_{p,j}$ is the stiffness of the jth ruling line as found from Eq. (11).

Knowing the angular displacement of each individual unit facilitates the stress analysis on the torsion bars. Finding this angle is relatively straightforward for parallel ruling lines of generalized cylinders because the angular displacements of the individual units sum to the angular displacement of the entire array in bending. However, in the case of generalized cones and tangent developed surfaces, the combined angular displacement of the individual units is not equal to the angular displacement of the array.

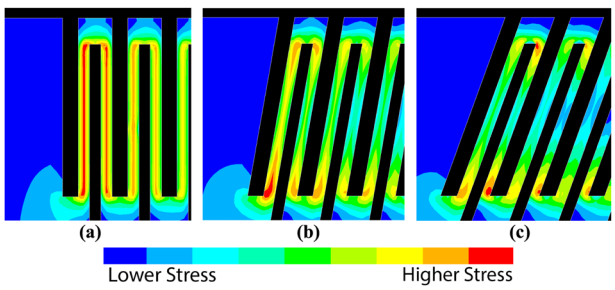

Fig. 9 Von Mises stress contours of the (*a*) 0 degree offset model, (*b*) 10 degree offset model, and (*c*) 20 degree offset model

For a generalized cylinder with parallel arrangements of the same stiffness (i.e., constant K_p) and equal spacing between the parallel arrangements, the relationship between the total angular displacement of the array, Θ, and the angular displacement of a parallel arrangement (which is also the displacement of an individual unit, θ) is described by

$$\theta = \frac{\Theta}{n+1} \tag{13}$$

where n is the number of ruling lines containing joints.

For a generalized cone with parallel arrangements of the same stiffness (constant K_p), and equal spacing, the relationship between the total angular sweep of the formed array in degrees, Θ as shown in Fig. 10, and the angular displacement of any parallel arrangement in degrees, θ, is dependent upon not only n, the number of ruling lines containing joints, but also γ, the angle swept by the planar undeveloped cone as shown in Fig. 11. To facilitate simplicity in the formulas, let

$$\xi = \cos^2\left(\frac{\gamma}{2n+2}\right) + \frac{\cos\left(\frac{\gamma}{n+1}\right) - 1}{2\tan^2\left(\frac{\Theta}{2n+2}\right)} \tag{14}$$

The angle of any parallel arrangement in degrees, θ, which is also the displacement of the individual units in the arrangement can be described as

$$\theta = 180 - \arccos\left(\frac{(\xi-1) + (-1-\xi)\cos\left(\frac{\Theta}{n+1}\right)}{(\xi+1) + (1-\xi)\cos\left(\frac{\Theta}{n+1}\right)}\right) \tag{15}$$

The geometry of the formed cone where R is the radius of the formed cone and H is the height of the formed cone can be related to ξ and r, the radius of the planar undeveloped cone as shown in Fig. 11, by

$$R = r(1-\xi)^{\frac{1}{2}} \tag{16}$$

$$H = r(\xi)^{\frac{1}{2}} \tag{17}$$

If the number of joints containing ruling lines is allowed to approach infinity, then the angular displacement of the joints on the ruling lines, θ, goes to zero and the expression for ξ becomes

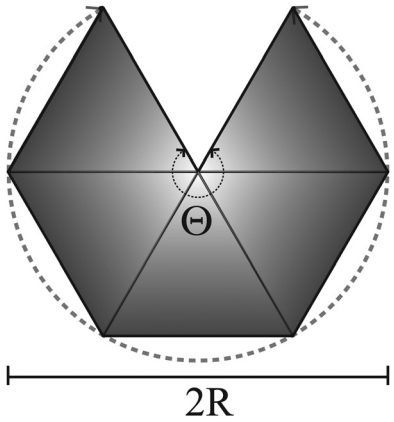

Fig. 10 Definition of the total angular displacement of a partially formed cone

Downloaded From: http://asmedigitalcollection.asme.org/ on 03/07/2016 Terms of Use: http://www.asme.org/about-asme/terms-of-use

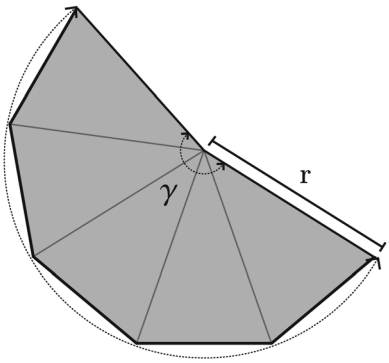

Fig. 11 Parameters of the planar undeveloped cone

$$\xi = 1 - \frac{\gamma^2}{\Theta^2} \tag{18}$$

5 Conical Array Pattern Generation

A technique to generate an array pattern for a conical developable surface using torsional joints is explained in this section. The product of this technique is a network of lines that provide a cut pattern which will form the array. When using the technique the designer is allowed to choose a minimum torsion bar width, which is often one of the critical dimensions in determining the stress present in the developed surface. Using the selected minimum torsion bar width, the technique finds a pattern which maximizes the amount of ruling lines containing torsion joints as well as maximizing the length of the torsion bars in order to minimize the stress present in the developed conical structure.

The steps to generating a conical array pattern are as follows:

- First the designer needs to select a radius for the hole which will be at the top of the cone. As ruling lines collect toward a focal point, interference between hinges will occur if the hole is not present. As the hole becomes larger more torsion bars can be placed in the pattern near the top of the cone and lower stresses will result. Let this radius be called r_1.
- Next the number of repeating units, N, in the cut pattern (as shown in Fig. 12) should be preliminarily selected. The minimum width of the torsion bars, $w_{\min}$, can be found by applying the Law of Cosines with the result

$$w_{\min} = r_1\left(2 - 2\cos\left(\frac{\gamma}{N}\right)\right)^{\frac{1}{2}} \tag{19}$$

where γ is the angle swept by the planar undeveloped cone. The number of repeating units, and consequently the minimum width, can be selected based on the amount of expected deflection of each individual unit in conjunction with a stress analysis of a rectangular bar in torsion.

- More levels of cuts can be introduced along the ruling lines as shown in Fig. 13. The radii of the circles at which these cuts can be introduced are described by

$$r_i = r_1\left(\frac{1 - \cos\left(\frac{\gamma}{N}\right)}{1 - \cos\left(\frac{\gamma}{2^{(i-1)}N}\right)}\right)^{\frac{1}{2}} \tag{20}$$

where r_i is the ith level radius.

- Once these lines have been generated to the desired radius, the designer must choose where to preserve material to create a continuous structure while maintaining the desired stiffness. At least one connection must be made between the repeating units to provide continuity, while more can be put into the pattern to increase resistance to parasitic in-plane movement of the surface. Figure 14 shows examples of two patterns where material is preserved to provide continuity. The outermost edge cut of the repeating unit can be interrupted at any point and similar interruptions can occur on at most every other cut line across the pattern to maintain the function of the torsional units. Also, triangular cuts rather than linear cuts can be made to cause the minimum torsion bar width to be utilized as much as possible in the design.

6 Structure and Mechanism Examples

Subtractive and additive manufacturing techniques can be used to create structures and mechanisms using lamina emergent arrays in a variety of materials. The arrays can vary widely in appearance depending upon the requirements of each application. When selecting attributes of the arrays, such as n and m, the type of LEM used as the fundamental unit, and the geometry of the fundamental unit itself, it is useful for the designer to consider factors such as the required displacement of the surface, the material being used, the thickness of the material, and aesthetics. These factors dictate the stress developed in the surface and will help the designer select array attributes which will enable the array to function without failure.

6.1 Subtractive Manufacturing. Subtractive manufacturing techniques such as milling, etching, laser cutting, and waterjet cutting can be used to create the lamina emergent arrays in a planar sheet. The two-dimensional geometry in the following four developable structures was created with a laser cutter.

Figure 15(*a*) shows a cylinder made of 2.54 mm (0.1 in.) cold press illustration board using the mixed tension resistant joint. A cone made of 4.8 mm (0.19 in.) cherry plywood is shown in (*b*). This cone uses torsional parallel joints to enable deployment motion and the cut pattern was generated using the technique

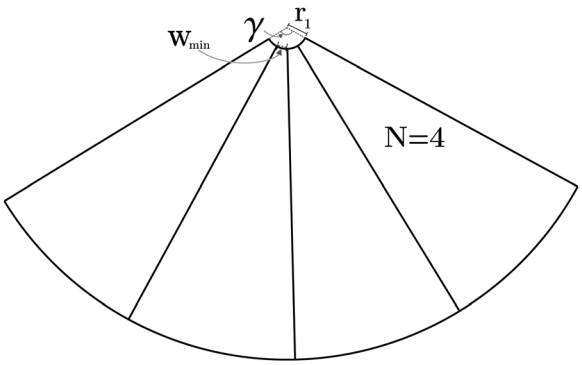

Fig. 12 Initial geometry of conical cut pattern generation

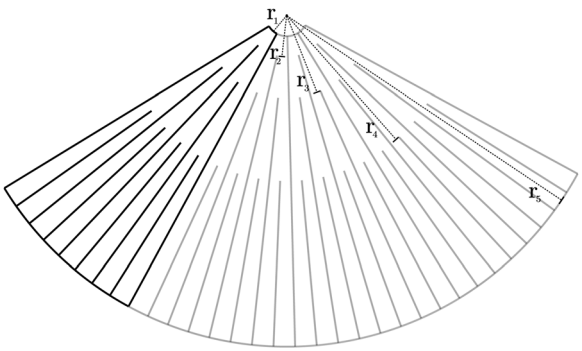

Fig. 13 Introducing additional levels of cuts

Downloaded From: http://asmedigitalcollection.asme.org/ on 03/07/2016 Terms of Use: http://www.asme.org/about-asme/terms-of-use

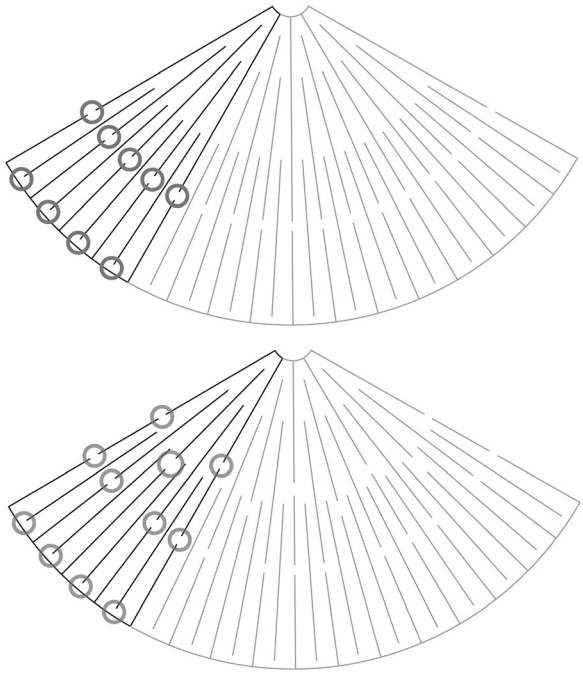

Fig. 14 Examples of cut patterns adjusted in the circled regions to preserve continuity

described in Sec. 5. For this cone, $\gamma = 100\,\text{deg}$ and $\Theta = 360\,\text{deg}$ with a radius $r = 16.17\,\text{cm}$ (6.37 in.) and inside hole radius $r_1 = 0.508\,\text{cm}$ (0.2 in.). Each ruling line containing a torsion bar is considered to be a ruling line with a joint giving $n = 80$. The number of repeating units was selected to be $N = 5$. These parameters are shown labeled on the cone in the flat state in Fig. 15. From these parameters, the height of the formed cone can be calculated as $H = 15.5\,\text{cm}$ (6.11 in.) from Eqs. (14) and (17), the formed radius as $R = 4.49\,\text{cm}$ (1.77 in.) from Eqs. (14) and (16), and the minimum width of a torsion bar as $w_{\min} = 1.76\,\text{mm}$ (0.069 in.) from Eq. (19).

Figures 16 and 17 show curved-fold origami models designed by the author Lang, which have been transitioned into thick material [6]. The model shown in Fig. 16 is "Crashing Volcanoes" made of 0.292 cm (0.115 in.) acrylic with a fabric backing. This model consists of four conical developable patches which are joined by splicing together ruling lines and reflecting ruling lines over a conic line. A single LET joint was patterned in series across the developable patches to maximize the torsion bar lengths and thus reduce stress in the structure.

The design can be analyzed by separately considering the two distinct conical patches, the outside edge patch and inside patch. The parameters for these conical patches are shown in Table 1. In determining n, the number of ruling lines containing joints, each torsion bar is considered as a joint. For the outside edge patch, n is observed to be 44. For the inside patch a group of torsion bars near both ends of the conical patch were intentionally made short to noticeably stiffen the structure in these regions. The resulting number of ruling lines containing joints was therefore reduced for the inside patch to account for these stiffer ends by only counting torsion bars which had longer torsion bar lengths, resulting in $n = 20$. Assuming each of the torsion bars has the same angular displacement allows for the computation of the angular displacement of each joint unit using Eq. (15). Note that the planar undeveloped radius, r, is not required to compute the displacement of each of the torsion bars. Once again disregarding the stiffer portions of the inside red patch, the geometry of the smallest length torsion bar in both patches is used to calculate the maximum torsion stress, $\tau_{\max}$, induced by the joint displacement using equations for torsion of rectangular beams [39]. Table 1 reports the material properties used, where G is the shear modulus of the acrylic and S_{sy} is the material's shear yield stress.

Figure 17 is Lang's origami model Elliptic Infinity transitioned into 2.692 mm (0.106 in.) medium density fiber-board and 22.86 μm (0.9 mils) metallic glass to create the creases. Metallic glass is an amorphous metal with properties that make it a suitable material for compliant structures [40]. The model Elliptic Infinity is based off of a single ellipse with ruling lines radiating from the focal points of the ellipse. The technique described in Sec. 5 was adjusted for each conical developable patch to create the pattern of torsion joints with hinge axes that match the ruling lines. The

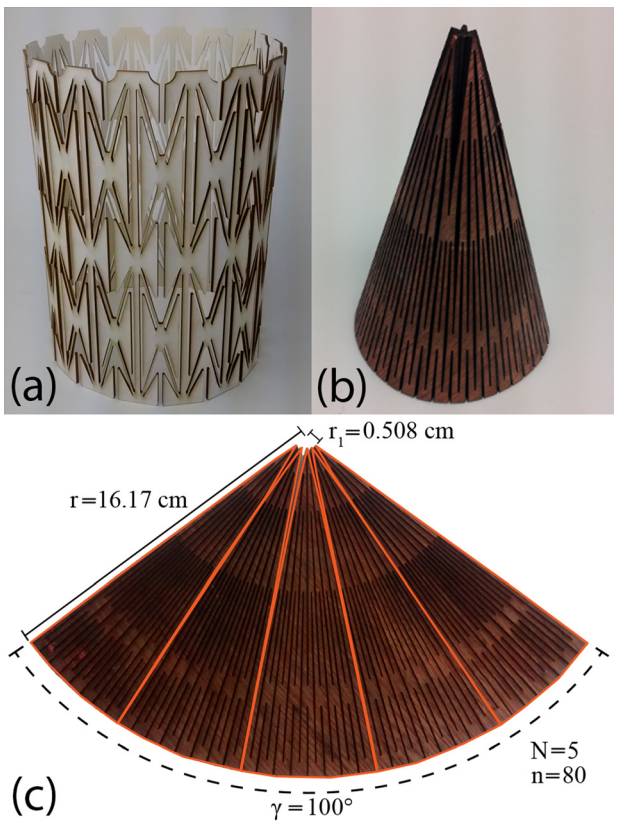

Fig. 15 Examples of lamina emergent arrays to create developable surfaces in materials other than paper: (*a*) cylinder, (*b*) cone, and (*c*) cone in the flat state with labeled parameters

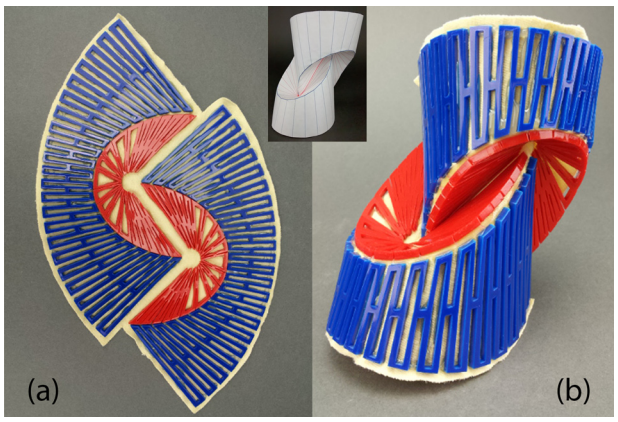

Fig. 16 Crashing volcanoes transitioned from paper (origami model is shown in the inset) to acrylic with a fabric backing in its (*a*) flat state and (*b*) deployed state

Downloaded From: http://asmedigitalcollection.asme.org/ on 03/07/2016 Terms of Use: http://www.asme.org/about-asme/terms-of-use

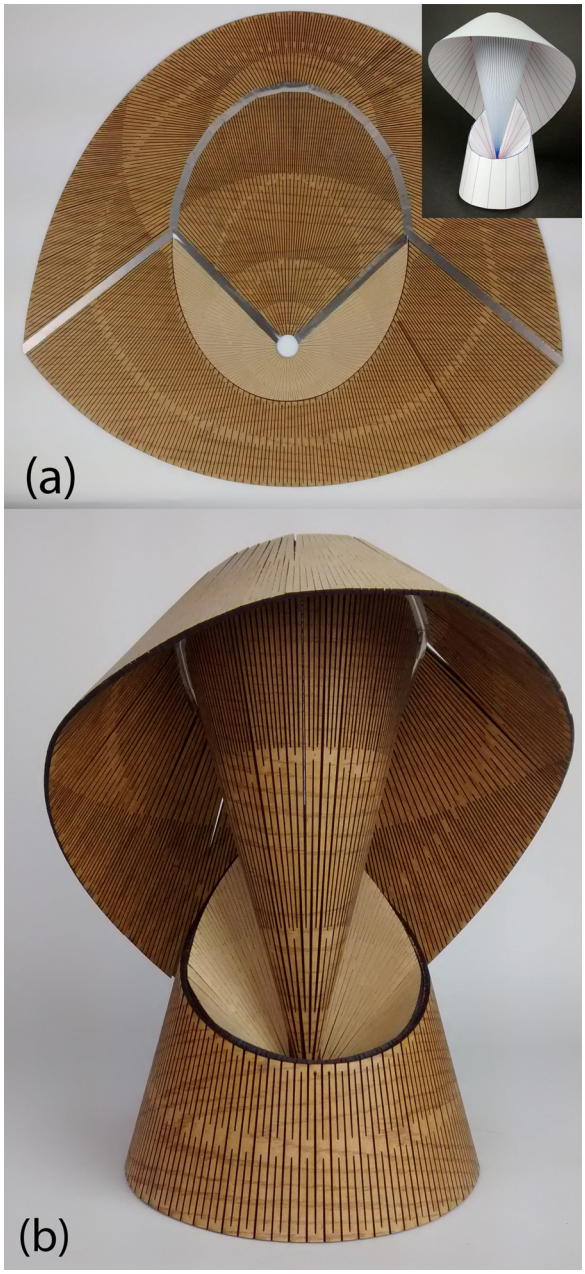

Fig. 17 Elliptic infinity transitioned from paper (origami model is shown in the inset) to particle board in its (*a*) flat state and (*b*) deployed state

structure in the flat state is approximately 50 cm (19.7 in.) wide by 43 cm (16.9 in.) tall with a deployed height of 30 cm (11.8 in.).

6.2 Additive Manufacturing (3D Printing). Additive manufacturing has commonly been used to create complex 3D shapes, yet it also has the ability to rapidly create lamina emergent arrays which can be designed to be folded or deployed into a specific shape. Recent research in 3D printing investigates not only how complex shapes can be accomplished with 3D printing but also how assembly and function can be facilitated through the use of multiple types of materials, deposition processes, and embedding materials [41,42]. The following two mechanisms show how developable origami patterns can be transitioned to thick materials using lamina emergent arrays by 3D printing flat designs which are biased to be assembled, or folded, into a certain structure.

The oriceps are an origami-inspired mechanism for use in robotic surgery applications where the instrument must be compact for entry into the body through small incisions and deployed to its functional state after entering the body [43]. The origami pattern used in the oriceps can be adapted to a curved crease pattern which is developable. A lamina emergent array of groove joints can be specified along the ruling lines and curved creases of the pattern. 3D printing was used to create this lamina emergent array as shown in Fig. 18(*a*) from polylactic acid (PLA) on a Makerbot Replicator 2. The compliant reduced cross-sectional area in the groove joints was created by printing two layers of PLA with the tool path orthogonal between the two

Table 1 Crashing volcanoes conical patch analysis

	Outside conical patch	Inside conical patch
Pattern parameters		
Θ	280 deg	280 deg
γ	96.38 deg	263.74 deg
n	44	20
Calculated joint displacement		
θ	5.84 deg	4.49 deg
Joint geometry		
L_T	1.20 cm (0.472 in.)	0.622 cm (0.245 in.)
t	0.180 cm (0.071 in.)	0.163 cm (0.064 in.)
w	0.292 cm (0.115 in.)	0.292 cm (0.115 in.)
Material properties		
G	1020 MPa (148 ksi)	1020 MPa (148 kpsi)
S_{sy}	38.5 MPa (5.59 ksi)	38.5 MPa (5.59 ksi)
Calculated max shear stress		
τ_{max}	13.7 MPa (2.00 ksi)	18.9 MPa (2.75 ksi)

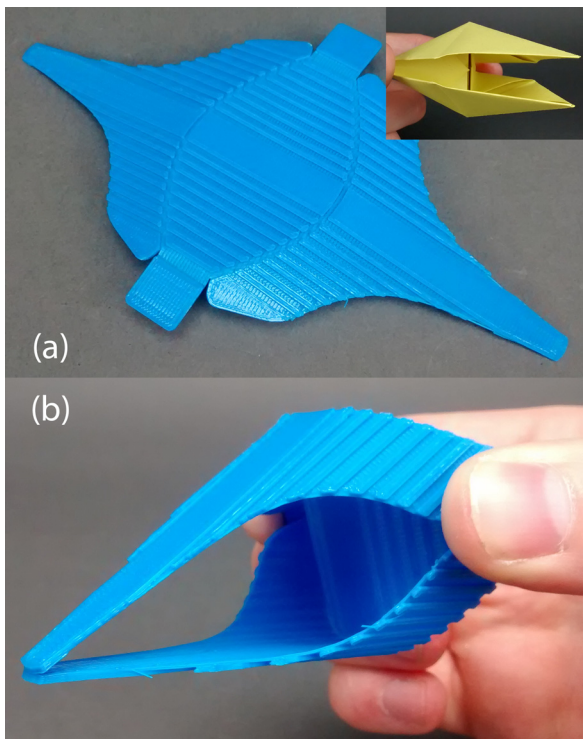

Fig. 18 3D printed curved-fold oriceps in its (*a*) flat printed state (origami model which provided inspiration is shown in the inset) and (*b*) folded, functional state

Downloaded From: http://asmedigitalcollection.asme.org/ on 03/07/2016 Terms of Use: http://www.asme.org/about-asme/terms-of-use

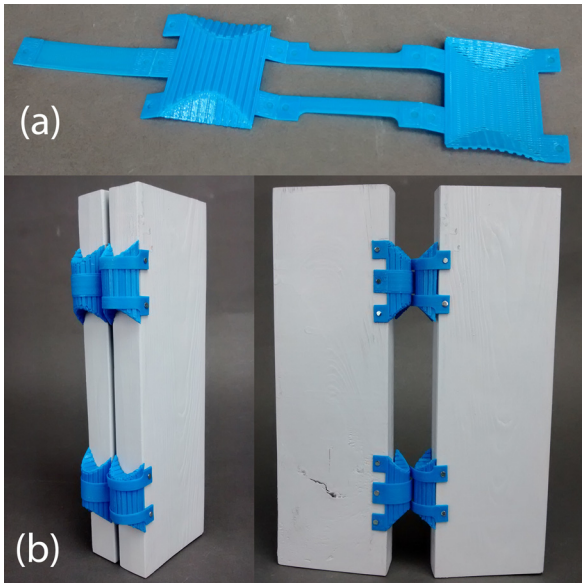

Fig. 19 3D printed D-CORES in (*a*) flat printed state and (*b*) folded state connecting two panels with nearly 360 degrees of rotation

layers. The build time was 25 min and required 5 g of PLA. The folded, functional oriceps are shown in Fig. 18.

The deployable compliant rolling contact element (D-CORE) is a curved-crease inspired mechanism which can be planar manufactured and folded into its functional state as a compliant rolling hinge [44]. Groove joints were placed upon the ruling lines and curved creases of this design similar to the oriceps pattern and the flat pattern was 3D printed. Each D-CORE required 3 g of material and 17 min to print in its flat configuration shown in Fig. 19(*a*). The joints were folded and attached to rigid panels as shown in Fig. 19(*b*). With the D-CORE hinges the panels can undergo nearly 360 deg of rotation. The hinged panels from Fig. 19(*b*) were compressively loaded with the panels 180 deg from each other. The hinges failed at a load of approximately 220 N (49.5 pounds).

7 Conclusion

This research has demonstrated a method to create developable structures suited to deployable applications by implementing arrays of lamina emergent joints. Furthermore, the alignment of the axes of these joints to the ruling lines of the surface has been shown to be an efficient configuration in terms of stress reduction in the structure and bias the structure to fold and deploy along a specific path. A mathematical model was developed for finding the stiffness of these types of structures as well as for computing the angular displacement of surfaces with parallel ruling lines and ruling lines which meet at a focus. A technique for generating a cut pattern for a generalized cone was laid out. Using these ideas, several example pieces were created.

Using lamina emergent arrays with joint axes aligned to ruling lines provides a vehicle for transitioning curved-fold origami patterns to engineering materials. These ideas can progress applications where storage space is a constraint, such as in devices for minimally invasive surgery, aerospace, and portable outdoor equipment. Particular possible applications include folding antennae, emergency shelters, flexible decorative or functional paneling, morphing surfaces such as wings on unmanned air vehicles (UAVs), and conformable protective equipment. Using arrays of lamina emergent joints enables a designer to decouple certain material properties from the modulus of the material. For example, electrical conductivity and the modulus of a material generally increase with each other, but using lamina emergent arrays it may be possible to construct a highly flexible panel that is also electrically conductive.

While this paper outlines methods for constructing cylindrical and conical surfaces from lamina emergent arrays, future work may include the development of methods to design tangent developable surfaces suited to deployment and to incorporate other types of joints besides those investigated. Intentionally using joints which enable additional motions besides a primary folding motion can possibly facilitate double-curvature or approximately developable shapes to be realized from planar materials. Panels which can stretch and shear in plane, a commonly desired characteristic in applications such as morphing wings, may also be possible. In addition, further methods can be developed in generating conical arrays which enable a designer to begin with various parameters, such as a desired cone shape and maximum stress, and calculate the remaining parameters.

Acknowledgment

This material is based on work supported by the National Science Foundation and the Air Force Office of Scientific Research under NSF Grant No. EFRI-ODISSEI-1240417 and by the National Science Foundation Graduate Research Fellowship Program under Grant No. 1247046.

References

[1] Struik, D. J., 1961, *Lectures on Classical Differential Geometry*, 2nd ed., Addison-Wesley, Reading, MA.
[2] Cajori, F., 1929, "Generalizations in Geometry as Seen in the History of Developable Surfaces," Am. Math. Mon., **36**(8), pp. 431–437.
[3] Lawrence, S., 2011, "Developable Surfaces: Their History and Application," Nexus Network J., **13**(3), pp. 701–714.
[4] Pottmann, H., and Wallner, J., 2009, *Computational Line Geometry*, Springer Science & Business, Heidelberg, Germany.
[5] Ushakov, V., 1999, "Developable Surfaces in Euclidean Space," J. Aust. Math. Soc. (Ser. A), **66**(3), pp. 388–402.
[6] Lang, R. J., 2013, "One Ellipse to Rule Them All," The Fold (Origami USA), Nov.–Dec. (epub).
[7] Fuchs, D., and Tabachnikov, S., 1999, "More on Paperfolding," Am. Math. Mon., **106**(1), pp. 27–35.
[8] Solomon, J., Vouga, E., Wardetzky, M., and Grinspun, E., 2012, "Flexible Developable Surfaces," Comput. Graphics Forum, **31**(5), pp. 1567–1576.
[9] Bo, P., and Wang, W., 2007, "Geodesic-Controlled Developable Surfaces for Modeling Paper Bending," Comput. Graphics Forum, **26**(3), pp. 365–374.
[10] Rose, K., Sheffer, A., Wither, J., Cani, M.-P., and Thibert, B., 2007, "Developable Surfaces From Arbitrary Sketched Boundaries," Fifth Eurographics Symposium on Geometry Processing (SGP '07), Barcelona, Spain, July 4–6, pp. 163–172.
[11] Demaine, E. D., Demaine, M. L., Koschitz, D., and Tachi, T., 2011, "Curved Crease Folding: A Review on Art, Design and Mathematics," IABSE-IASS Symposium, London, Sept. 20–23, Paper No. 10065184.
[12] Huffman, D. A., 1976, "Curvature and Creases: A Primer on Paper," IEEE Trans. Comput., **25**(10), pp. 1010–1019.
[13] Resch, R. D., 1974, "Portfolio of Shaded Computer Images," Proc. IEEE, **62**(4), pp. 496–502.
[14] Duncan, J. P., and Duncan, J., 1982, "Folded Developables," Proc. R. Soc. London A, **383**(1784), pp. 191–205.
[15] Demaine, E. D., Demaine, M. L., and Koschitz, D., 2011, "Reconstructing David Huffman's Legacy in Curved-Crease Folding," Origami5, pp. 39–51.
[16] Demaine, E. D., Demaine, M. L., Huffman, D. A., Koschitz, D., and Tachi, T., 2014, "Designing Curved-Crease Tessellations of Lenses: Qualitative Properties of Rulings," 6th International Meeting on Origami in Science, Mathematics and Education (OSME 2014), Tokyo, Aug. 10–13, Paper No. 168.
[17] Koschitz, R. D., 2014, "Computational Design With Curved Creases: David Huffman's Approach to Paperfolding," Ph.D. thesis, Massachusetts Institute of Technology, Cambridge, MA.
[18] Jacobsen, J. O., Winder, B. G., Howell, L. L., and Magleby, S. P., 2010, "Lamina Emergent Mechanisms and Their Basic Elements," ASME J. Mech. Rob., **2**(1), p. 011003.
[19] Howell, L. L., 2001, *Compliant Mechanisms*, Wiley, New York.
[20] Delimont, I. L., Magleby, S. P., and Howell, L. L., 2015, "Evaluating Compliant Hinge Geometries for Origami-Inspired Mechanisms," ASME J. Mech. Rob., **7**(1), p. 011009.
[21] Delimont, I. L., 2014, "Compliant Joints Suitable for Use as Surrogate Folds," Master's thesis, Brigham Young University, Provo, UT.
[22] Jacobsen, J. O., Chen, G., Howell, L. L., and Magleby, S. P., 2009, "Lamina Emergent Torsional (LET) Joint," Mech. Mach. Theory, **44**(11), pp. 2098–2109.
[23] You, Z., 2014, "Folding Structures Out of Flat Materials," Science, **345**(6197), pp. 623–624.
[24] Dureisseix, D., 2012, "An Overview of Mechanisms and Patterns With Origami," Int. J. Space Struct., **27**(1), pp. 1–14.
[25] Jamal, M., Bassik, N., Cho, J.-H., Randall, C. L., and Gracias, D. H., 2010, "Directed Growth of Fibroblasts Into Three Dimensional Micropatterned Geometries Via Self-Assembling Scaffolds," Biomaterials, **31**(7), pp. 1683–1690.

Downloaded From: http://asmedigitalcollection.asme.org/ on 03/07/2016 Terms of Use: http://www.asme.org/about-asme/terms-of-use

[26] Silverberg, J. L., Evans, A. A., McLeod, L., Hayward, R. C., Hull, T., Santangelo, C. D., and Cohen, I., 2014, "Using Origami Design Principles to Fold Reprogrammable Mechanical Metamaterials," Science, **345**(6197), pp. 647–650.
[27] Lee, D.-Y., Kim, J.-S., Kim, S.-R., Koh, J.-S., and Cho, K.-J., 2013, "The Deformable Wheel Robot Using Magic-Ball Origami Structure," ASME DETC2013-13016.
[28] Ma, J., and You, Z., 2014, "Energy Absorption of Thin-Walled Square Tubes With a Prefolded Origami Pattern—Part I: Geometry and Numerical Simulation," ASME J. Appl. Mech., **81**(1), p. 011003.
[29] Liu, Y., Boyles, J. K., Genzer, J., and Dickey, M. D., 2012, "Self-Folding of Polymer Sheets Using Local Light Absorption," Soft Matter, **8**(6), pp. 1764–1769.
[30] Felton, S., Tolley, M., Demaine, E., Rus, D., and Wood, R., 2014, "A Method for Building Self-Folding Machines," Science, **345**(6197), pp. 644–646.
[31] Saito, K., Pellegrino, S., and Nojima, T., 2014, "Manufacture of Arbitrary Cross-Section Composite Honeycomb Cores Based on Origami Techniques," ASME J. Mech. Des., **136**(5), p. 051011.
[32] Miyashita, S., DiDio, I., Ananthabhotla, I., An, B., Sung, C., Arabagi, S., and Rus, D., 2015, "Folding Angle Regulation by Curved Crease Design for Self-Assembling Origami Propellers," ASME J. Mech. Rob., **7**(2), p. 021013.
[33] Gattas, J. M., and You, Z., 2014, "Miura-Base Rigid Origami: Parametrizations of Curved-Crease Geometries," ASME J. Mech. Des., **136**(12), p. 121404.
[34] Chung, W., Kim, S.-H., and Shin, K.-H., 2008, "A Method for Planar Development of 3D Surfaces in Shoe Pattern Design," J. Mech. Sci. Technol., **22**(8), pp. 1510–1519.
[35] Kilian, M., Flöry, S., Chen, Z., Mitra, N. J., Sheffer, A., and Pottmann, H., 2008, "Curved Folding," ACM Trans. Graphics, **27**(3), p. 75.
[36] Pottmann, H., Schiftner, A., Bo, P., Schmiedhofer, H., Wang, W., Baldassini, N., and Wallner, J., 2008, "Freeform Surfaces From Single Curved Panels," ACM Trans. Graphics, **27**(3), paper number 76.
[37] Eigensatz, M., Kilian, M., Schiftner, A., Mitra, N. J., Pottmann, H., and Pauly, M., 2010, "Paneling Architectural Freeform Surfaces," ACM Trans. Graphics, **29**(4), paper number 45.
[38] Stevens, K. A., 1981, "The Visual Interpretation of Surface Contours," Artif. Intell., **17**(1), pp. 47–73.
[39] Young, W. C., Budynas, R. G., and Sadegh, A. M., 2012, *Roark's Formulas for Stress and Strain*, 8th ed., McGraw-Hill, New York.
[40] Homer, E. R., Harris, M. B., Zirbel, S. A., Kolodziejska, J. A., Kozachkov, H., Trease, B. P., Borgonia, J.-P. C., Agnes, G. S., Howell, L. L., and Hofmann, D. C., 2014, "New Methods for Developing and Manufacturing Compliant Mechanisms Utilizing Bulk Metallic Glass," Adv. Eng. Mater., **16**(7), pp. 850–856.
[41] Ma, R. R., Belter, J. T., and Dollar, A. M., 2015, "Hybrid Deposition Manufacturing: Design Strategies for Multimaterial Mechanisms Via Three-Dimensional Printing and Material Deposition," ASME J. Mech. Rob., **7**(2), p. 021002.
[42] Kim, C., Espalin, D., Cuaron, A., Perez, M. A., Lee, M., MacDonald, E., and Wicker, R. B., 2015, "Cooperative Tool Path Planning for Wire Embedding on Additively Manufactured Curved Surfaces Using Robot Kinematics," Journal of Mechanisms and Robotics, **7**(2), p. 021003.
[43] Edmondson, B. J., Bowen, L. A., Grames, C. L., Magleby, S. P., Howell, L. L., and Bateman, T. C., 2013, "Oriceps: Origami-Inspired Forceps," ASME Paper No. SMASIS2013-3299.
[44] Nelson, T. G., Lang, R. J., Magleby, S. P., and Howell, L. L., 2015, "Curved-Folding-Inspired Deployable Compliant Rolling-Contact Element (D-CORE)," Mech. Mach. Theory (in press).

Downloaded From: http://asmedigitalcollection.asme.org/ on 03/07/2016 Terms of Use: http://www.asme.org/about-asme/terms-of-use